Electronic Supporting Information

Optical and electronic properties of different thin-film polymorphs of PDIF-CN_2 controlled by zone-casting conditions

Niklas J. Herrmann,[a] Nadine von Coelln,[a] Robin M. Teichgreber,[b] Sebastian Höfener,[c] Christian Huck,[a] Farhad Ghalami,[c] Simon Settele,[a] Manuel Hertzog,[a] Marcus Elstner,[cd] Petra Tegeder,[a] Eva M. Herzig,[b] and Jana Zaumseil*[a]

[a] Institute for Physical Chemistry, Heidelberg University, Heidelberg, Germany

[b] Institute of Physics, University of Bayreuth, Bayreuth, Germany

[c] Institute of Physical Chemistry, Karlsruhe Institute of Technology, Germany

[d] Institute of Biological Interfaces (IBG-2), Karlsruhe Institute of Technology, Germany

* Corresponding author email: *zaumseil@uni-heidelberg.de*

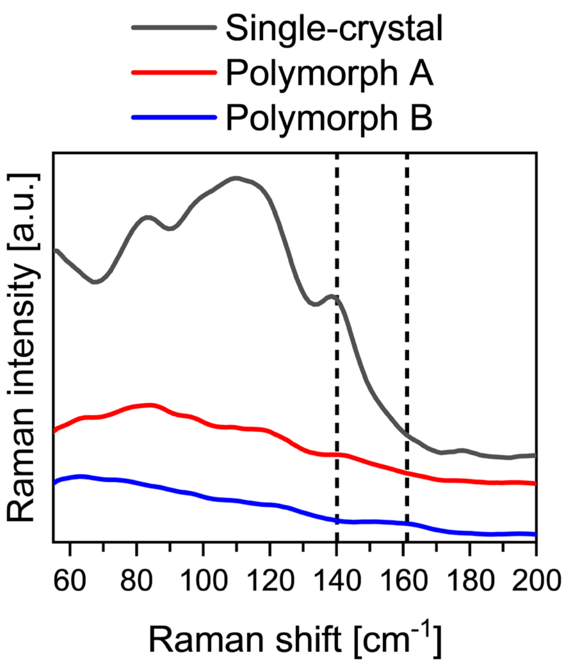

Figure S1. Stacked Raman spectra without baseline correction as collected from PDIF-CN_2 single crystal and thin films of PDIF-CN_2 (polymorphs A and B). Vertical lines highlight the two Raman modes that are markedly different for the two polymorphs.

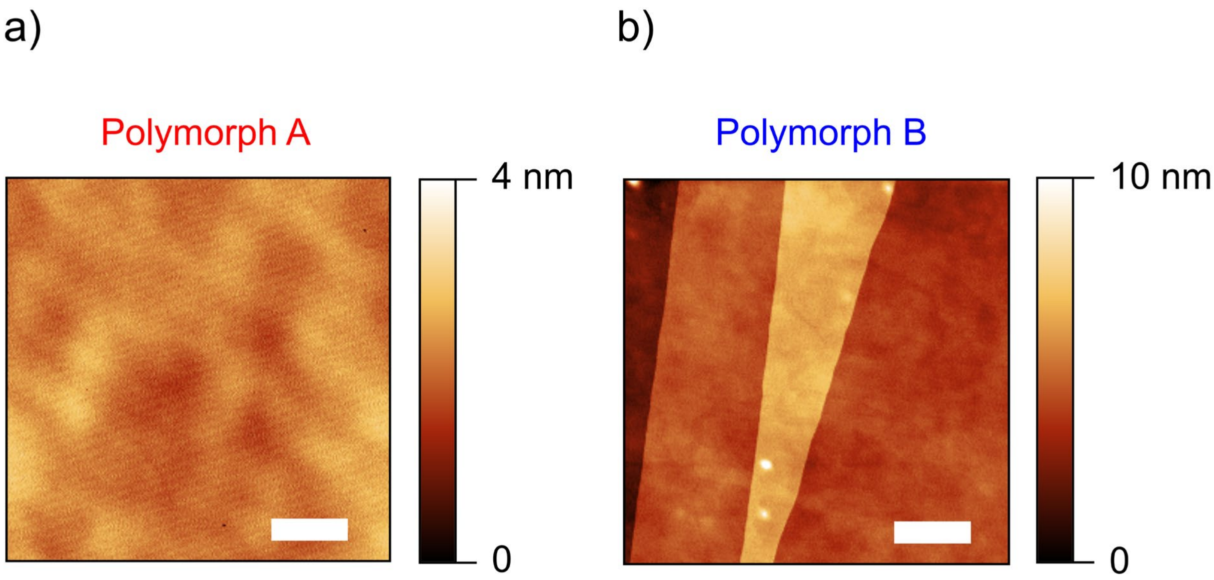

Figure S2. Atomic force microscopy images (ScanAsyst^{TM} mode) of zone-cast PDIF-CN_2 films of (a) polymorph A (rms 0.29 nm) and (b) polymorph B (rms 0.34 nm, step-height: 2 ± 0.2 nm). Images are 5x5 μm^2, scale bar 1 μm.

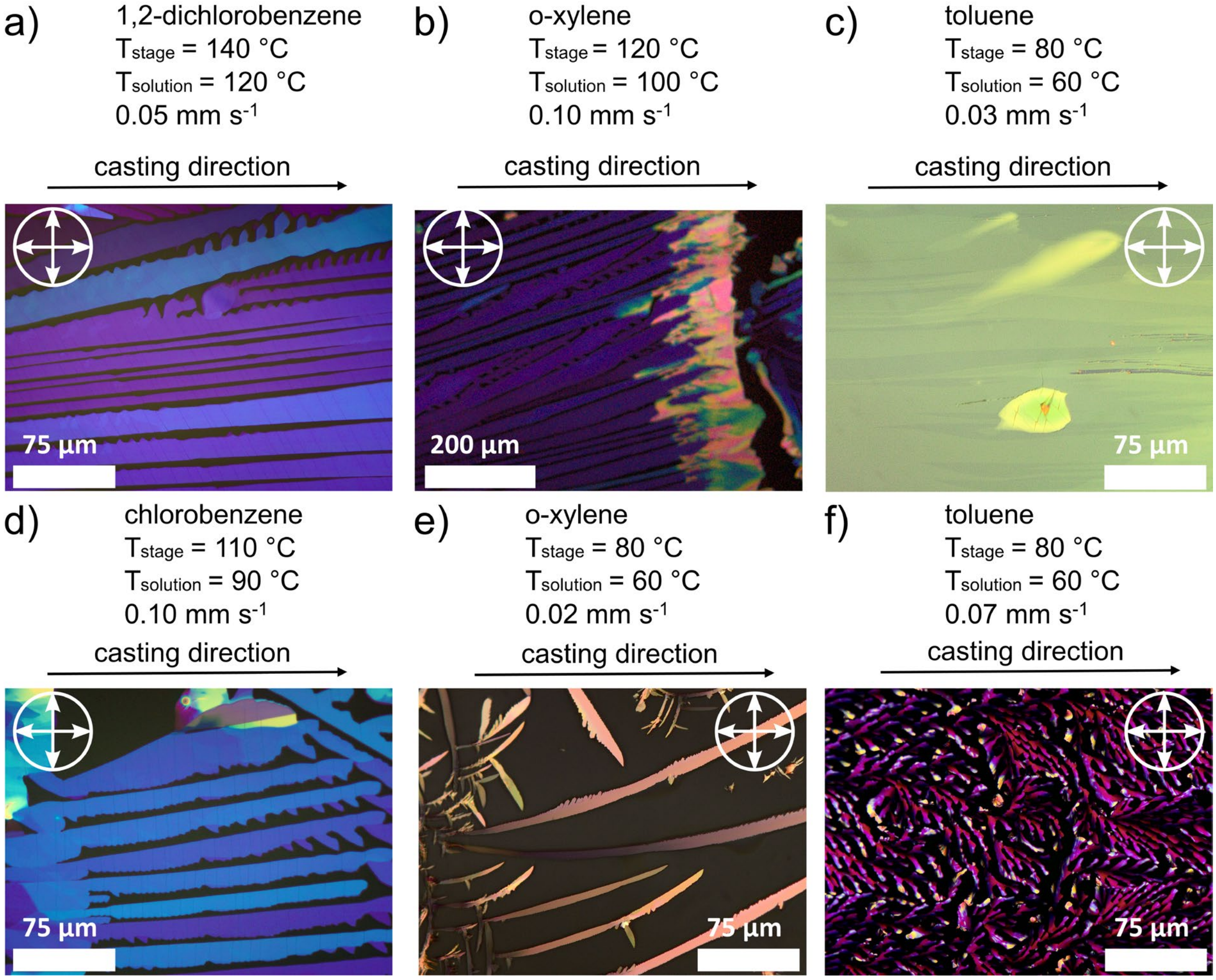

Figure S3. Cross-polarized optical microscope images of PDIF-CN_2 films that were zone-cast from different solvents under different conditions. Note, PDIF-CN_2 films a), b), d), f) were zone-cast on Si/SiO_2/BCB substrates.

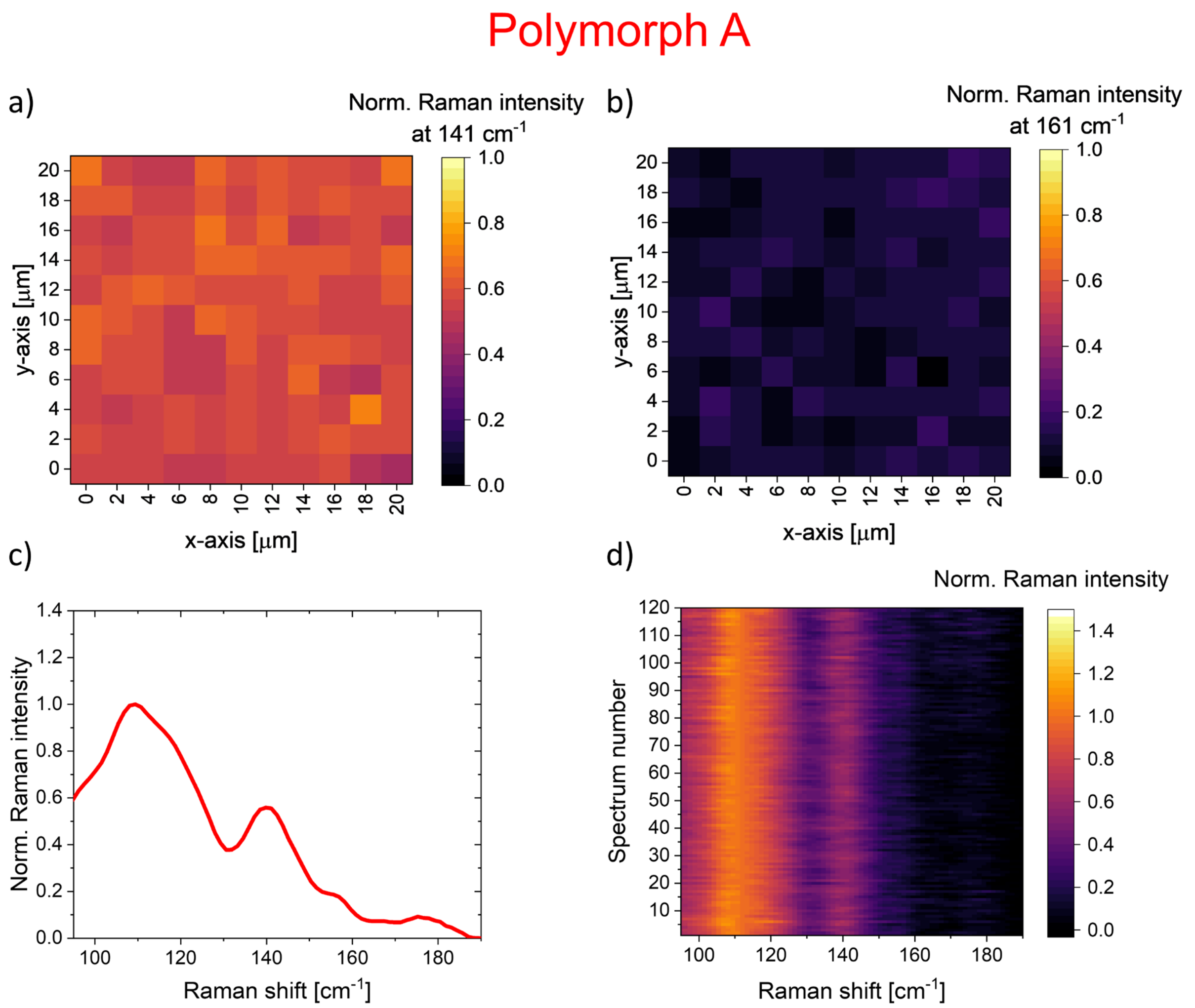

Figure S4. Thin film of PDIF-CN_2 zone-cast from o-xylene (polymorph A): Raman intensity maps over an area of 20 x 20 µm² at (a) 141 cm^{-1} and (b) 161 cm^{-1} normalized to the Raman signal at 114 cm^{-1}. Averaged and normalized Raman spectrum (c) and hyperspectral map (d) of the Raman data in (a) and (b), indicating a large and homogeneous area of only polymorph A.

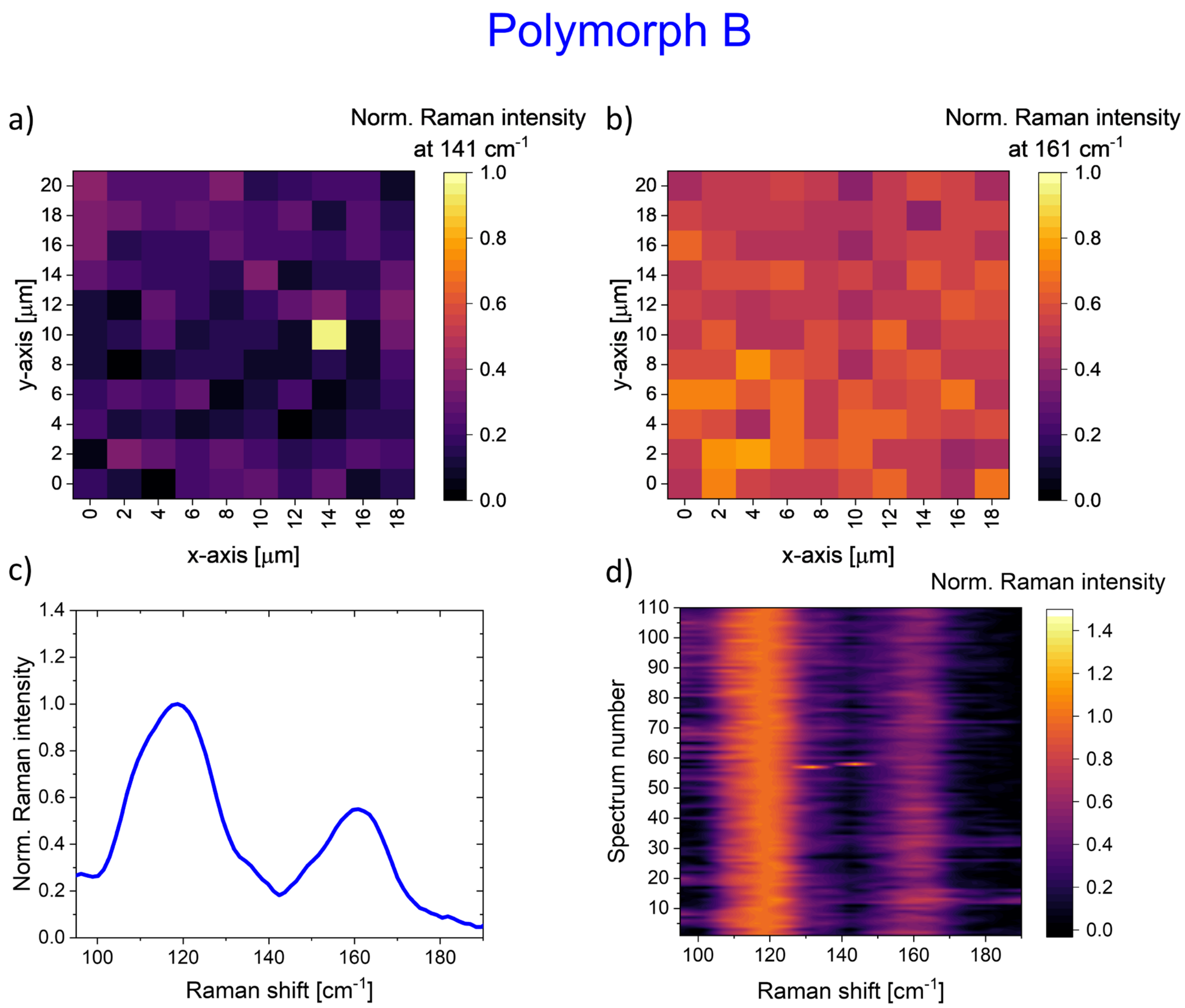

Figure S5. Thin film of PDIF-CN_2 zone-cast from toluene (polymorph B): Raman intensity maps over an area of 20 x 20 μm² at (a) 141 cm^{-1} and (b) 161 cm^{-1} normalized to the Raman signal at 119 cm^{-1}. Averaged and normalized Raman spectrum (c) and hyperspectral map (d) of the Raman data in (a) and (b), indicating a large and homogeneous area of only polymorph B.

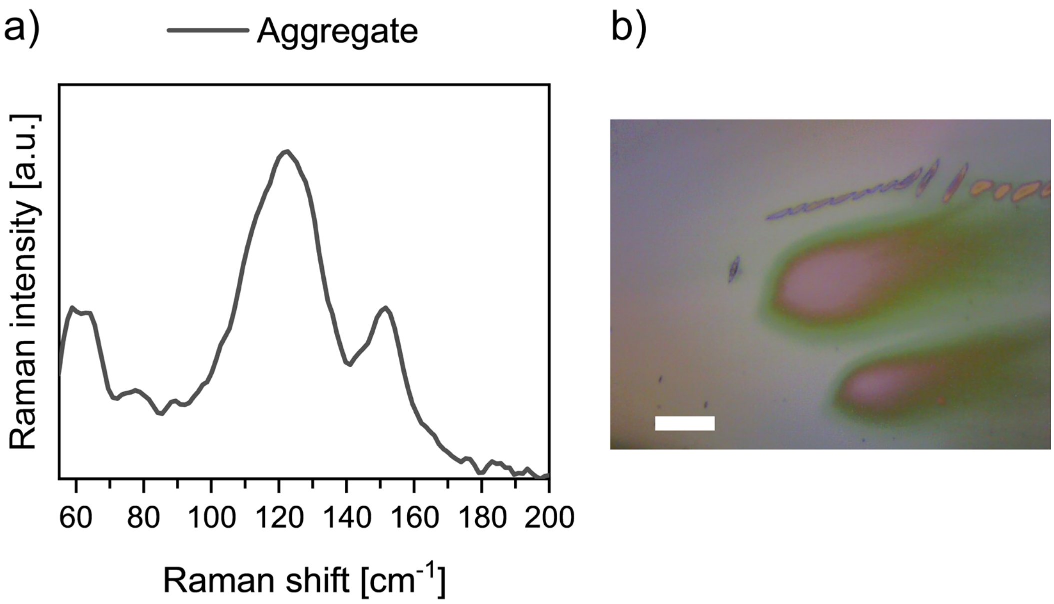

Figure S6. (a) Baseline corrected normalized Raman spectra of a teardrop-shaped aggregate in a thin-film zone-cast from toluene. (b) Microscope images of a teardrop-shaped aggregate, scale bar 20 μm.

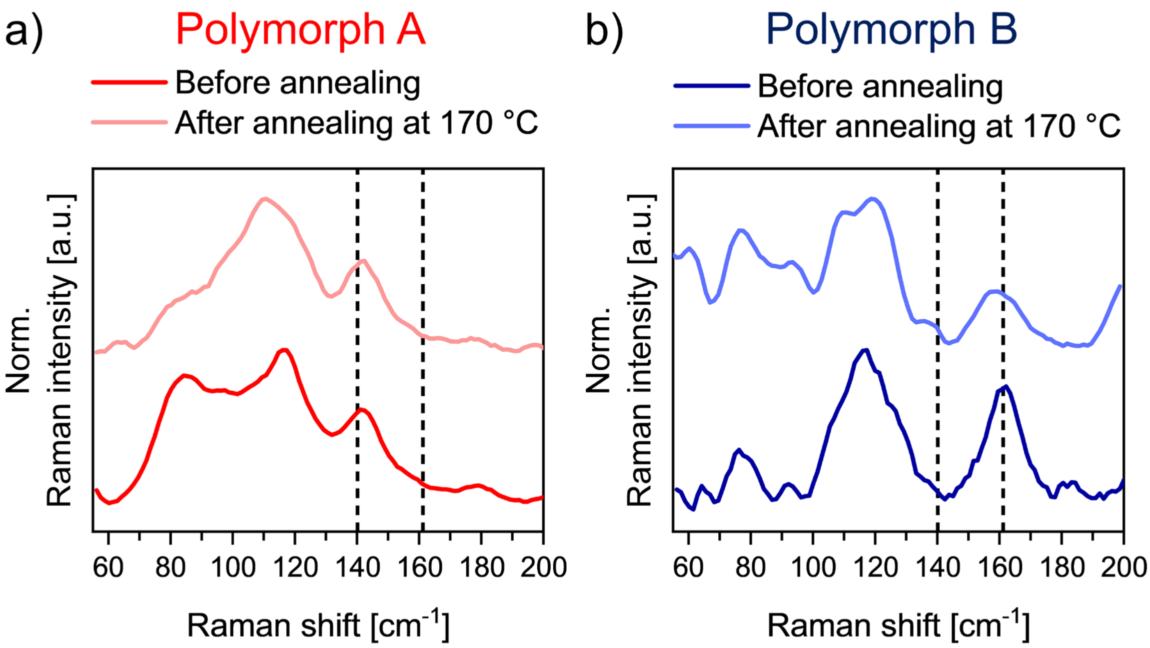

Figure S7. (a) Stacked, baseline corrected and normalized Raman spectra of thin-films of (a) polymorph A and (b) polymorph B before and after thermal annealing at 170 °C for 1 hour. Vertical lines highlight the two Raman modes that are markedly different for the two polymorphs.

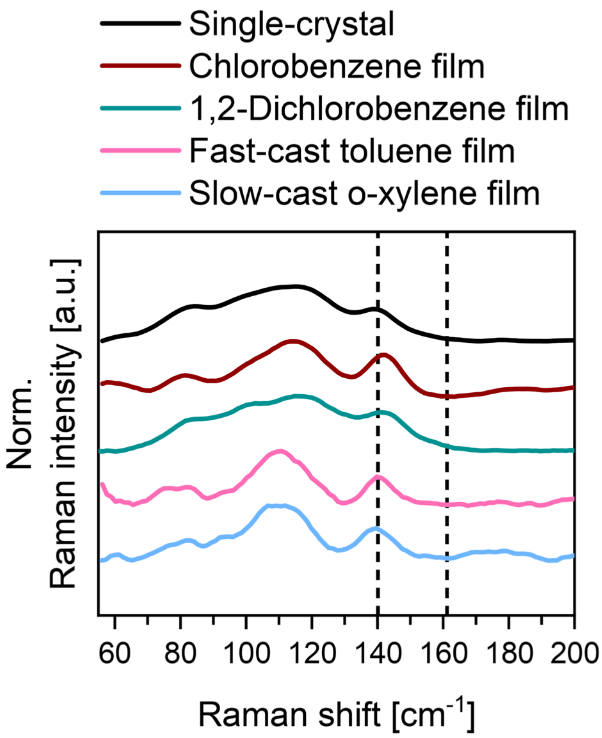

Figure S8. Stacked baseline corrected normalized Raman spectra collected from PDIF-CN_2 single-crystal and PDIF-CN_2 thin films deposited from chlorobenzene and 1,2-dichlorobenzene under the optimized casting conditions as shown in **Figure S3d** and **S3a** and from toluene and o-xylene under non-optimal conditions as shown in **Figure S3f** and **S3e**, respectively. Vertical lines highlight the two Raman modes that are markedly different for polymorph A and B.

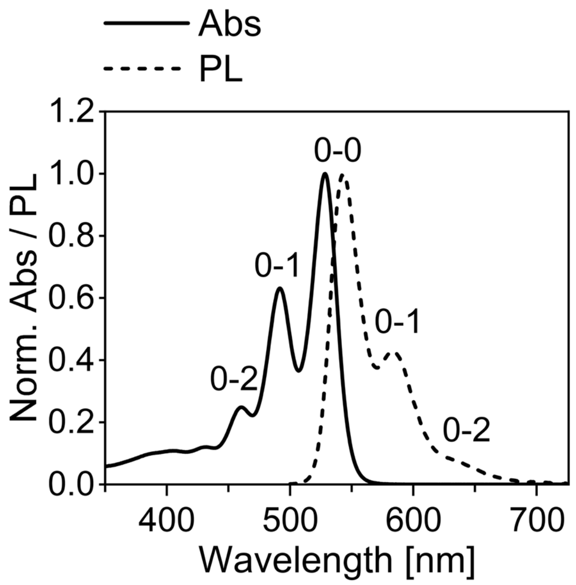

Figure S9. Normalized absorption (Abs) and photoluminescence (PL) spectrum of a dilute PDIF-CN_2 in toluene solution.

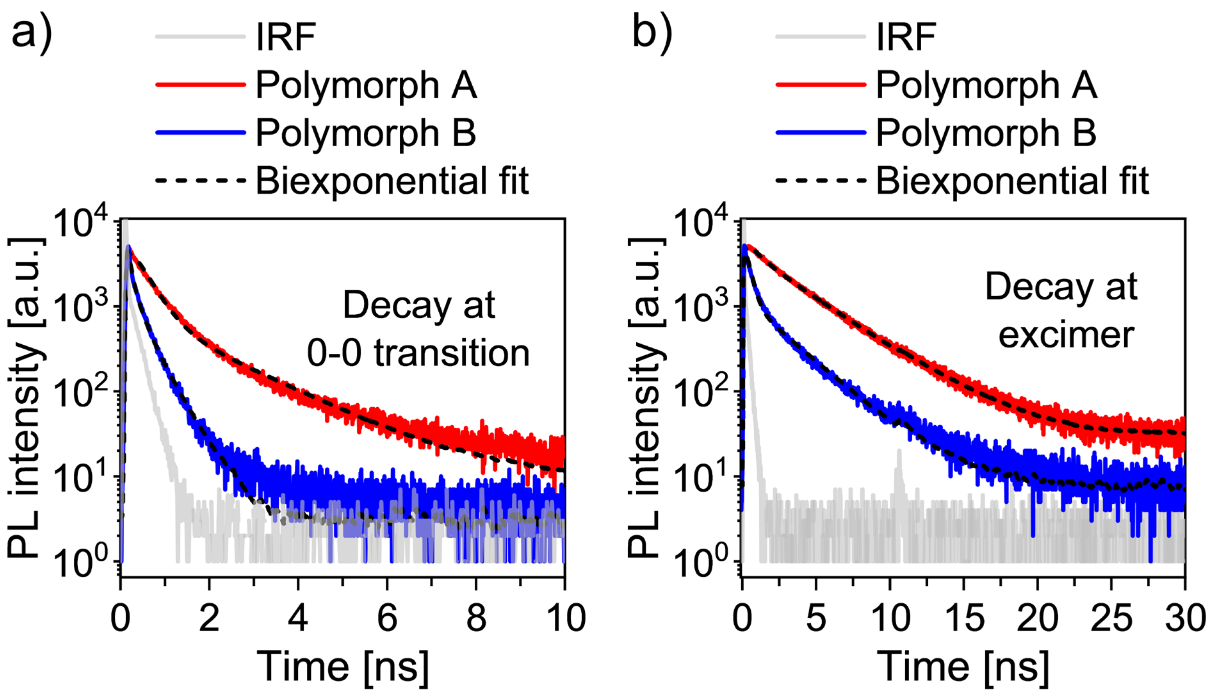

Figure S10. (a) TCSPC histograms of the photoluminescence decay of the 0-0 transition of polymorph A (red, emission at 615 nm) and polymorph B (blue, emission at 580 nm); (b) TCSPC histograms of the photoluminescence decay of the excimer emission of polymorph A (red, emission from 700 nm to 950 nm) and polymorph B (blue, emission from 700 nm to 950 nm). In all cases the time traces were fitted as a biexponential decay (black) with a re-convolution method including the instrument response function (IRF, gray).

Table S1. Extracted short and long lifetime components (τ_{short}, τ_{long}) and corresponding normalized amplitudes (A_{short}, A_{long}) for the PL emission of the 0-0 transition (polymorph A: 615 nm; polymorph B, 580 nm) and of the excimer (700 nm to 950 nm).

	Decay at 0-0-transition				Decay at excimer			
	A_{short} [%]	τ_{short} [ps]	A_{long} [%]	τ_{long} [ns]	A_{short} [%]	τ_{short} [ps]	A_{long} [%]	τ_{long} [ns]
Polymorph A	88	310	12	1.7	30	870	70	3.7
Polymorph B	93	72	7	0.49	84	300	16	2.9

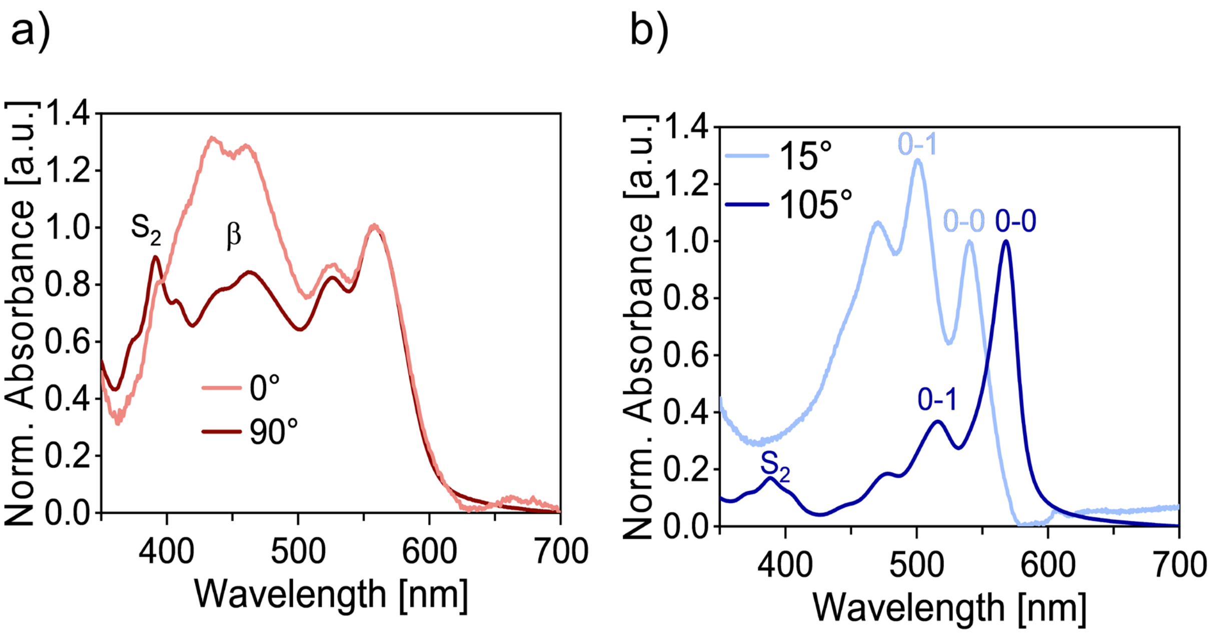

Figure S11. Normalized polarized UV-Vis absorption spectra of (a) polymorph A (PDIF-CN_2 zone-cast from o-xylene) and (b) polymorph B (PDIF-CN_2 zone-cast from toluene) with indicated angle of polarization versus casting direction.

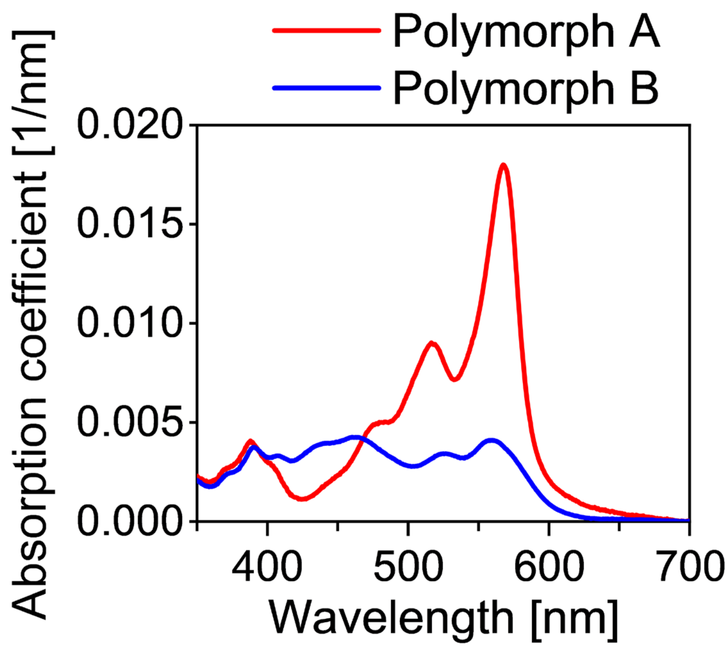

Figure S12. Absorption coefficients of thin films of polymorph A and B.

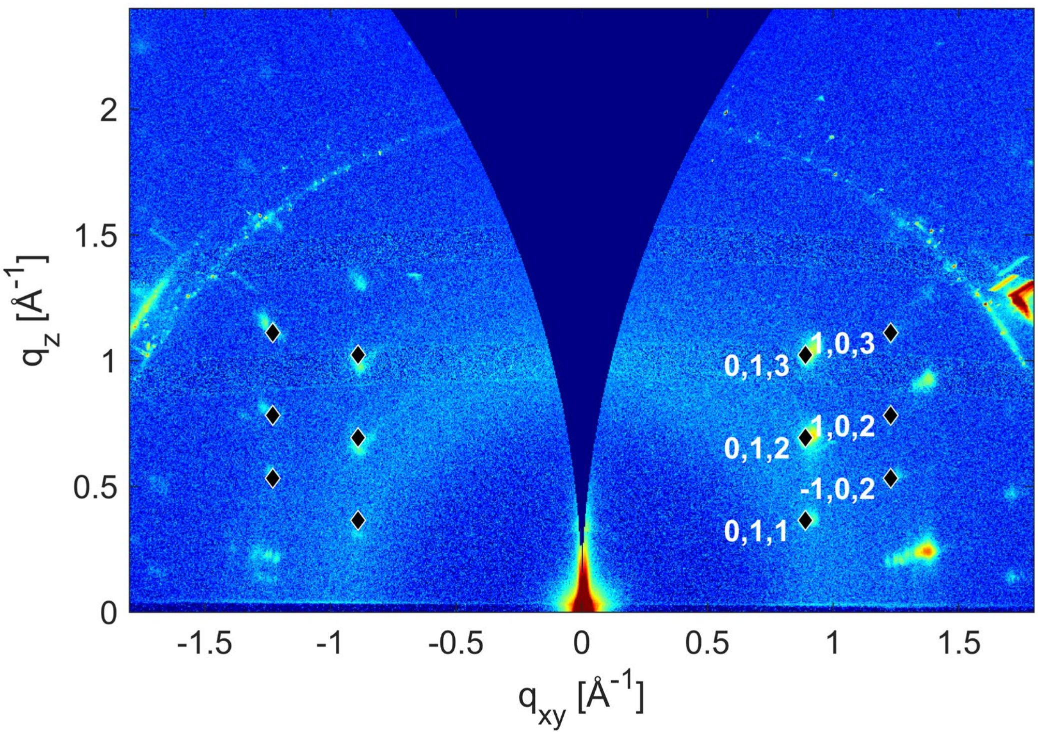

Figure S13. GIWAXS data of PDIF-CN2 film zone-cast from o-xylene collected over an angular range of 180° around an axis vertically perpendicular to the beam. Diffraction peak positions were calculated for unit cell parameters of polymorph A (◆) as shown in Table 1 (main manuscript). The associated crystal planes are labelled by their Miller indices.

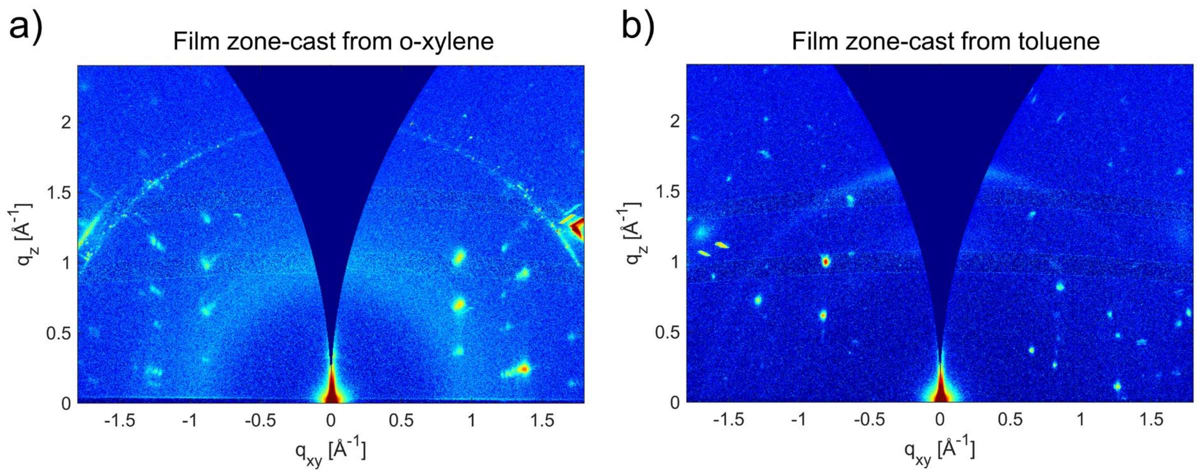

Figure S14. GIWAXS data of PDIF-CN2 films zone-cast from (a) o-xylene and (b) toluene collected over an angular range of 180° around an axis vertically perpendicular to the beam.

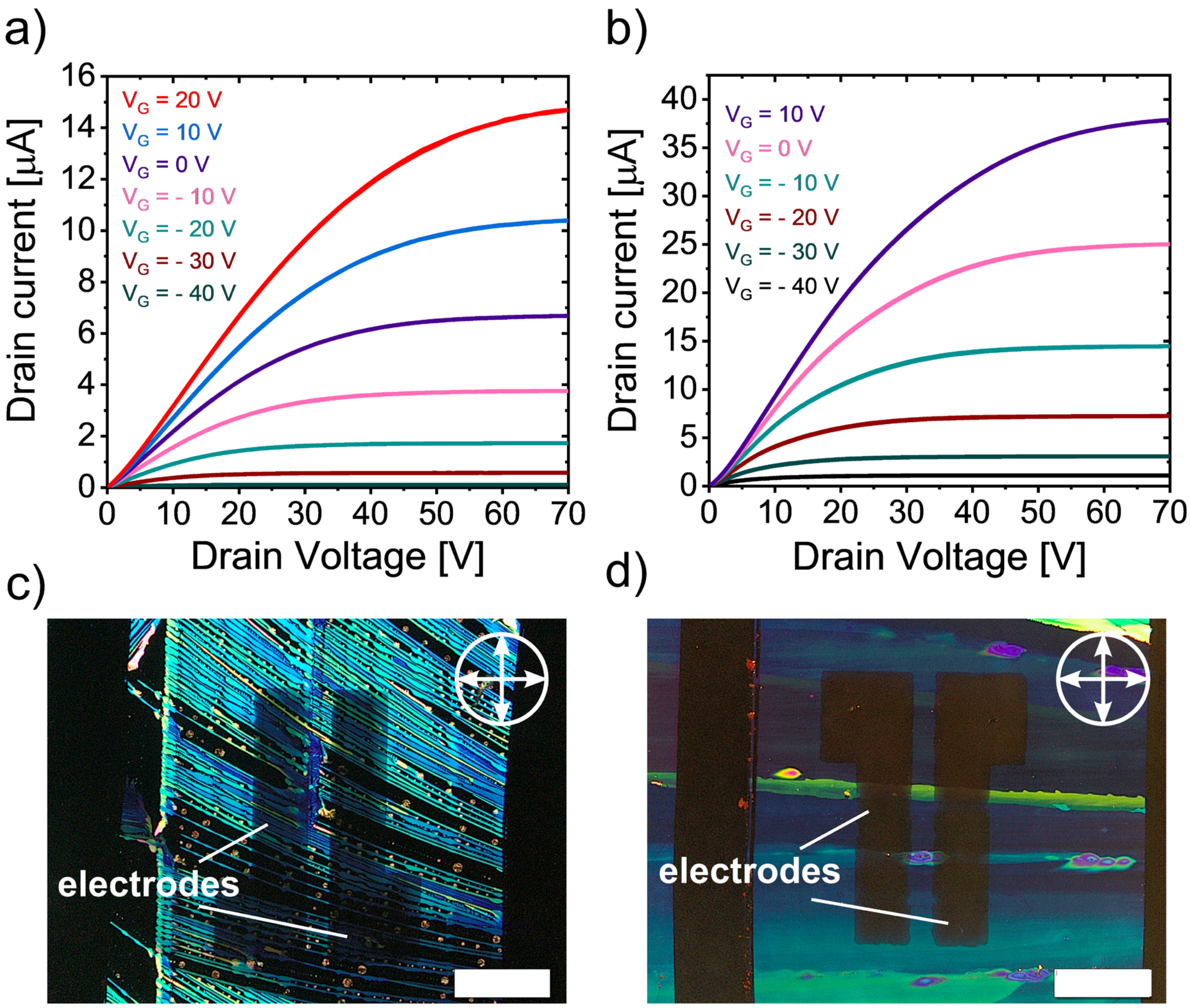

Figure S15. Representative output curves of bottom-gate, top-contact transistors of (a) polymorph A and (b) polymorph B and cross-polarized microscope images of the corresponding transistors (c) and (d), scale bar 500 μm.